

Effect of Frequency on the Iron Losses of 0.5% and 1.5% Si Nonoriented Electrical Steels

Marcos F. de Campos¹, Taeko Yonamine¹, Marcos Fukuhara¹, Fernando J. G. Landgraf², Carlos A. Achete^{1,3}, and Frank P. Missell^{1,4}

¹Instituto Nacional de Metrologia, Normalização, e Qualidade Industrial—Inmetro, Duque de Caxias, RJ 25250-020, Brazil

²Departamento de Engenharia Metalúrgica e de Materiais, Escola

Politécnica, Universidade de São Paulo, São Paulo, SP 05508-970, Brazil

³COPPE, Universidade Federal do Rio de Janeiro, Rio de Janeiro, RJ 21941-972, Brazil

⁴Universidade de Caxias do Sul, Caxias do Sul, RS 95070-560, Brazil

The effect of grain size on iron losses were compared for two electrical steels with 0.5 and 1.5 wt% Si. The results confirm that the optimum grain size for minimizing the energy losses decreases when the electrical resistivity decreases or when the frequency increases. Experimental results are compared to a model which considers the influence of grain size. The recrystallization texture of the alloys varies little with grain size and consists mainly of the fibers $\{111\}\langle uvw \rangle$ and $\langle 110 \rangle // RD$.

Index Terms—Electrical steels, grain size, loss modeling, texture.

I. INTRODUCTION

ELECTRICAL steels are widely used industrial materials, for example, as the core of motors or in transformers. Nonoriented steels are applied in rotating machines, and should have ideally random texture, of type $\{100\}\langle 0vw \rangle$, i.e., with the easy magnetization axis of body-centered cubic (bcc) iron parallel to the plane of the sheet, randomly distributed.

Aside from texture, another factor which influences losses in electrical steels is grain size. Several authors [1], [2] have pointed out the existence of an optimum grain size for minimization of losses. A model [3], based on both theoretical and experimental data, predicted that the optimum grain size for minimizing the energy losses decreases as: electrical resistivity decreases or frequency increases or thickness of steel sheet increases. The objective of this paper is to test the validity of that model in different circumstances, including in steels with different Si content (i.e., different resistivities) and with measurements performed over a larger frequency range and for different magnetic inductions. Although frequencies of 50–60 Hz are typical for most applications of electrical steels, operating frequencies of 400 Hz are encountered in aircraft [4]. Thus, another useful characteristic of the model [3] is providing insight into the loss behavior of steels at other frequencies.

II. EXPERIMENT

Two alloys were studied: 1) alloy A with 0.52 wt% Si, and resistivity = $20.5 \mu\Omega\text{-cm}$; and 2) alloy B with 1.53 wt% Si and resistivity = $32.2 \mu\Omega\text{-cm}$. Both alloys received different “skin-passes” (4–12% reduction in thickness), which resulted in different recrystallized grain sizes, after an annealing at 760 °C. Magnetic measurements were done in a Brockhaus model MPG 100D hysteresis measuring system (with Epstein frame), in the frequency range of 1–400 Hz, for a magnetic induction $B =$

1.5 T. The magnetic measurements at quasistatic condition were made at a frequency of 5 mHz, also for a magnetic induction $B = 1.5$ T. The texture was measured in a FEI Quanta 200 scanning electron microscope (SEM) equipped with a TSL system for electron backscattered diffraction (EBSD) analysis. The average grain size was measured parallel to the transverse section of the sheet, by the intercept method.

III. RESULTS AND DISCUSSION

The grain size was introduced as a variable using a simple metallurgical rule [5]: With increasing deformation (i.e., increasing thickness reduction), the energy stored during the deformation is greater, resulting in a larger number of recrystallization nuclei and a lower final recrystallized grain size. However, as the samples were submitted to different reductions, the thickness of samples is an additional variable; but, its effect can be separated in the model [3], by assuming that the anomalous loss component depends on the square of the thickness [6], [7].

A. Brief Description of the Model

According to the loss separation procedure, the total losses P_t are separated into three components

$$P_t = P_h + P_{cl} + P_{an} \quad (1)$$

where P_{cl} is the classical eddy-current losses, P_{an} is the anomalous or excess losses, and P_h is the hysteresis losses, i.e., P_h is the area of the hysteresis curve in the quasistatic mode times the frequency f

$$P_h = f \oint B dH \quad (2)$$

where B is magnetic induction and H is the applied magnetic field. If we suppose that the area of the hysteresis curve in the

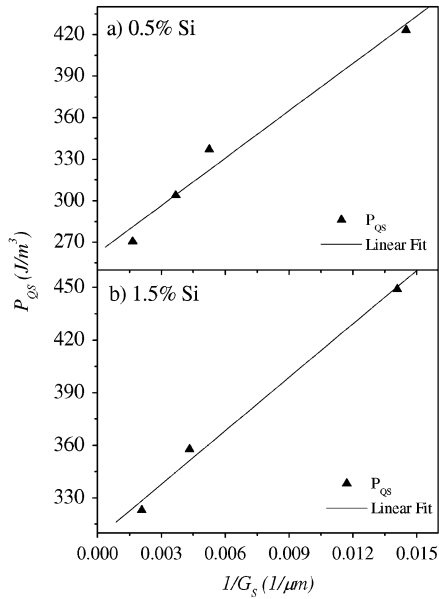


Fig. 1. Quasistatic losses P_{QS} versus grain size for (a) steel A and (b) steel B.

quasistatic mode is proportional to the inverse of the grain size G_s [3], [8], [9], then (2) becomes

$$P_h = \left(a_1 + \frac{a_2}{G_s} \right) \cdot B_{\max}^q \cdot f \quad (3)$$

where B_{\max} is the maximum induction and q is the Steinmetz exponent, with typical value $q = 1.6$ [3]. a_1 and a_2 are constants to be experimentally determined. The classical eddy losses P_{cl} are given [10], [11] by

$$P_{cl} = \frac{\pi^2 f^2 B_{\max}^2 e^2}{6\rho} \quad (4)$$

where e is the thickness of the sheet and ρ is the resistivity. The deduction of the equation for the anomalous losses P_{an} has been previously described [3]. It was assumed that the anomalous loss component depends on the square of the thickness [6], [7]

$$P_{an} = a_3 \cdot G_s^{1/2} \cdot \frac{1}{\rho} \cdot e^2 \cdot B_{\max}^2 \cdot f^{3/2} \quad (5)$$

where a_3 is a constant to be experimentally determined. The optimum grain size $G_{s_{op}}$ for minimizing the losses is

$$G_{s_{op}} = \left(\frac{a_4 \cdot \rho}{B_{\max}^{2-q} \cdot e^2 \cdot f^{1/2}} \right)^{2/3} \quad (6)$$

where $a_4 = (2a_2/a_3)$.

B. Comparison of the Model With Experimental Data

Fig. 1 shows that both alloys have an almost linear dependence of quasistatic loss P_{QS} with grain size, as expected from (6). P_{QS} (or H_c) $\propto \gamma/M_s G_s$, where γ is the domain wall energy, M_s is the saturation magnetization and H_c is the coercive field. The slope for both steels is quite similar, because γ/M_s is very nearly the same for both compositions.

Figs. 2 and 3, where loss separation was applied according (1), show that the optimum grain size changes with frequency,

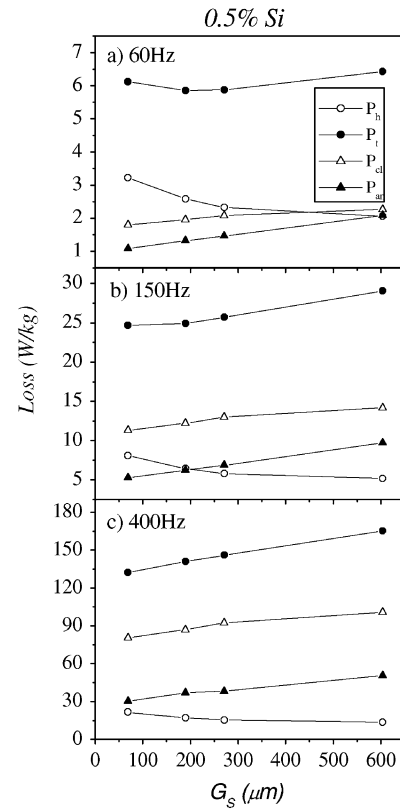


Fig. 2. Loss components versus grain size for steel A (0.5 wt% Si) for (a) 60 Hz, (b) 150 Hz, and (c) 400 Hz.

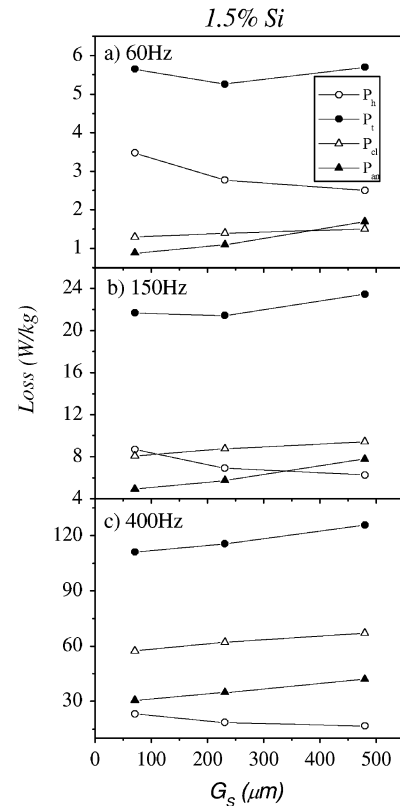


Fig. 3. Loss components versus grain size for steel B (1.5 wt% Si), for (a) 60 Hz, (b) 150 Hz, (c) 400 Hz.

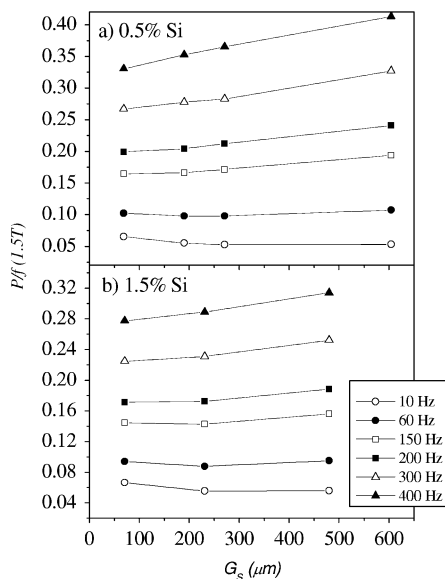


Fig. 4. Graph Pt/f (total losses/frequency) as a function of grain size for frequencies $f = 10, 60, 150, 200, 300,$ and 400 Hz. We clearly see that optimum grain size decreases when frequency increases.

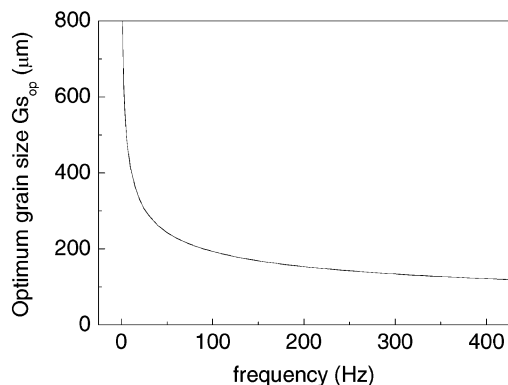


Fig. 5. Optimum grain size as a function of frequency, as estimated with the model, for steel B (1.5 wt% Si).

and that for higher resistivities $G_{s_{op}}$ tend to be lower. This can be modeled by means of (6), which predicts that the optimum grain size is higher for an alloy with more silicon (and higher resistivity), in agreement with the experimental results (50 Hz) of Shimanaka *et al.* [12], who showed that the optimum grain size is in the range 100–150 μm for steels with 1.85 to 3.2% Si. Fig. 4 shows that, increasing the frequency, the losses increase more pronouncedly for the steel with lower resistivity. The results of applying the model for steel B (1.5 wt% Si) were: 1) $f = 60$ Hz, $G_{s_{op}} = 230$ μm , 2) $f = 150$ Hz, $G_{s_{op}} = 170$ μm , and 3) $f = 400$ Hz, $G_{s_{op}} = 120$ μm , as shown in Fig. 5. The recrystallized grains of our sheets have a “pancake” shape, i.e., are much larger parallel to the transverse section of the sheet, than for the longitudinal section. This should explain the difference in relation to Shimanaka *et al.* [12], who probably reported the average grain size taking into account all the directions. In our case, the grain size was measured parallel to the surface which is preferable due the physical assumptions of the model [3].

The texture of the samples is quite similar, with two fibers $\langle 111 \rangle // \text{ND}$ (ND = normal direction) and $\langle 110 \rangle // \text{RD}$ (RD =

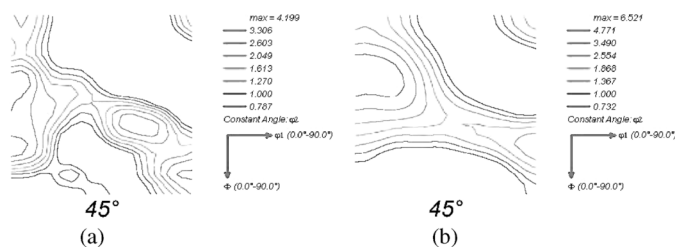


Fig. 6. Orientation distribution function (ODF) section $\varphi_2 = 45^\circ$ for steel A (0.5 wt% Si) samples with (a) grain size 604 μm and (b) grain size 69 μm . Bunge notation.

rolling direction) as the main texture components, almost not affected by grain size (see Fig. 6). However, the sample with the larger grain size [see Fig. 6(a)], has more Goss $\langle 110 \rangle [001]$ component and, presumably, better magnetic properties near the rolling direction. The texture is very similar to the other commercial nonoriented silicon steels [13], and is far from the ideal texture $\{100\} \langle 0vw \rangle$.

IV. CONCLUSION

Experimental data indicates that the optimum grain size for minimizing the iron losses changes with frequency and resistivity. A model to predict the optimum grain size, taking into account variables such as sheet thickness, resistivity, frequency, and maximum induction has been described. The recrystallization texture of our samples presents two fibers $\langle 111 \rangle // \text{ND}$ and $\langle 110 \rangle // \text{RD}$ as main components.

ACKNOWLEDGMENT

This work was supported in part by the Brazilian agency Conselho Nacional de Desenvolvimento Científico e Tecnológico (CNPq). The authors M. F. de Campos, T. Yonamine, and M. Fukuhara would like to thank CNPq-PROMETRO for their support. The authors would like to thank L. Gomes for quantitative metallography measurements.

REFERENCES

- [1] K. Matsumura and B. Fukuda, *IEEE Trans. Magn.*, vol. MAG-20, no. 5, pp. 1533–1538, Sep. 1984.
- [2] M. Shiozaki and Y. Kurosaki, *J. Mater. Eng.*, vol. 11, pp. 37–43, 1989.
- [3] M. F. de Campos, J. C. Teixeira, and F. J. G. Landgraf, *J. Magn. Magn. Mater.*, vol. 301, pp. 94–99, 2006.
- [4] L. M. C. Mhango and R. Perryman, *IEE Proc.-Electr. Power Appl.*, vol. 144, pp. 149–157, 1997.
- [5] J. E. Burke and D. Turnbull, *Progress in Metal Physics*. London, U.K.: Pergamon Press, 1952, vol. 3B, pp. 220–292.
- [6] E. T. Stephenson, *J. Appl. Phys.*, vol. 57, pp. 4226–4228, 1985.
- [7] D. C. Jiles, *Introduction to Magnetism and Magnetic Materials*. London, U.K.: Chapman & Hall, 1991.
- [8] E. Adler and H. Pfeiffer, *IEEE Trans. Magn.*, vol. MAG-10, no. 2, pp. 172–174, Jun. 1974.
- [9] J. Degauque, B. Astie, J. L. Porteseil, and R. Vergne, *J. Magn. Magn. Mater.*, vol. 26, pp. 261–263, 1982.
- [10] J. J. Thomson, *Electrician*, vol. 28, pp. 599–600, 1892.
- [11] C. D. Graham Jr., *J. Appl. Phys.*, vol. 53, pp. 8276–8280, 1982.
- [12] H. Shimanaka, Y. Ito, K. Matsumura, and B. Fukuda, *J. Magn. Magn. Mater.*, vol. 26, pp. 57–64, 1982.
- [13] M. F. de Campos, F. J. G. Landgraf, I. G. S. Falleiros, G. C. Fronzaglia, and H. Kahn, *ISIJ Int.*, vol. 44, pp. 1733–1738, 2004.